# Dense Optical Flow Estimation from the Monogenic Curvature Tensor *

Di Zang[1], Lennart Wietzke[1], Christian Schmaltz[2], and Gerald Sommer[1]

[1] Department of Computer Science, Christian-Albrechts-University of Kiel, Germany
{zd,lw,gs}@ks.informatik.uni-kiel.de
[2] Faculty of Mathematics and Computer Science, Saarland University, Germany
schmaltz@mia.uni-saarland.de

**Abstract.** In this paper, we address the topic of estimating two-frame dense optical flow from the monogenic curvature tensor. The monogenic curvature tensor is a novel image model, from which local phases of image structures can be obtained in a multi-scale way. We adapt the combined local and global (CLG) optical flow estimation approach to our framework. In this way, the intensity constraint equation is replaced by the local phase vector information. Optical flow estimation under the illumination change is investigated in detail. Experimental results demonstrate that our approach gives accurate estimation and is robust against noise contamination. Compared with the intensity based approach, the proposed method shows much better performance in estimating flow fields under brightness variations.

**Key words:** Optical flow estimation, phase, monogenic curvature tensor

## 1 Introduction

Optical flow estimation is one of the key problems gathering the interest of researchers for decades in the computer vision community. It has a wide application in motion estimation, object recognition, tracking, surveillance and so on.

Various approaches have been proposed to estimate the optical flow. Significant improvements [1] have been obtained since the pioneering work of Horn and Schunck [2] and Lucas and Kanade [3]. In [4], Barron et al. made the performance evaluation of optical flow techniques. The local phase-based method [5] was proven to be the best performed due to its subpixel accuracy and its robustness with respect to smooth contrast changes and affine deformations. Differential methods, on the other hand, have become the most frequently used techniques for optical flow estimation because of the simplicity and good performance. Among the differential methods, there exist two classes. They are local methods such as that of the Lucas and Kanada and global methods such as that

* This work was supported by German Research Association (DFG) Graduiertenkolleg No. 357 (Di Zang), DFG grant So-320/4-2 (Lennart Wietzke and Christian Schmaltz) and DFG grant So-320/2-3 (Gerald Sommer).

of the Horn and Schunk. Local methods are known to be more robust under noise, while global approaches yield 100% dense flow fields. Hence, Bruhn et al. [6] proposed the combined local-global (CLG) approach to yield dense optical flow fields which is robust against noise.

In order to have accurate and robust estimation of dense optical flow fields against noise and brightness variation, we propose a novel approach based on the monogenic curvature tensor, a new image model. In contrast to the classical phase computation in [5], the monogenic curvature tensor can generate multi-scale local phases of image structures in a rotation invariant way. Thus, the proposed approach combines the advantages of the phase-based method and the CLG method. Experiments with synthetic and real image sequences demonstrate the favorable performance of the proposed method when compared with the related work.

## 2 Monogenic Curvature Tensor

The monogenic curvature tensor is a novel 2D image model, from which multi-scale local phases of image structures can be obtained in a rotation invariant way. It is well known that the local phase has the advantage of being invariant to the illumination change [7]. In this paper, we will adapt the CLG method to this framework for the dense optical flow estimation. Hence, a brief overview of the novel image model is given in this section.

### 2.1 Basis Functions

The monogenic curvature tensor consists of a curvature tensor and its conjugate part. By employing damped 2D spherical harmonics as basis functions, the monogenic curvature tensor is unified with a scale-space framework. An $n$th order damped 2D spherical harmonic $H_n$ in the spectral domain takes the following form

$$H_n(\rho, \alpha; s) = \exp(in\alpha)\exp(-2\pi\rho s) = [\cos(n\alpha) + i\sin(n\alpha)]\exp(-2\pi\rho s)\ , \quad (1)$$

where $\rho$ and $\alpha$ denote the polar coordinates in the Fourier domain, $s$ refers to the scale parameter. The damped 2D spherical harmonic is actually 2D spherical harmonic $\exp(in\alpha)$ combined with the Poisson kernel $\exp(-2\pi\rho s)$ [8]. The first order damped 2D spherical harmonic is basically identical to the conjugate Poisson kernel [8]. When the scale parameter is zero, it is exactly the Riesz transform [9].

### 2.2 Curvature Tensor and Its Conjugate Part

In order to evaluate the local phase information, the curvature tensor and its harmonic conjugate part are designed to capture the even and odd information of 2D image structures.

Designing the curvature tensor is motivated by the second fundamental theorem of the differential geometry, that is the second order derivatives or Hessian matrix which contains curvature information of the original signal. Let $f$ be a 2D signal, its Hessian matrix is correspondingly given by

$$H = \begin{bmatrix} f_{xx} & f_{xy} \\ f_{xy} & f_{yy} \end{bmatrix} , \tag{2}$$

where $x$ and $y$ are the Cartesian coordinates. According to the derivative theorem of the Fourier theory, the Hessian matrix in the spectral domain reads

$$\mathcal{F}\{H\} = \begin{bmatrix} -4\pi^2\rho^2 \frac{1+\cos(2\alpha)}{2} F & -4\pi^2\rho^2 \frac{\sin(2\alpha)}{2} F \\ -4\pi^2\rho^2 \frac{\sin(2\alpha)}{2} F & -4\pi^2\rho^2 \frac{1-\cos(2\alpha)}{2} F \end{bmatrix} , \tag{3}$$

where $F$ is the Fourier transform of the original signal $f$. It is obvious that angular parts of the second order derivatives in the Fourier domain are related to 2D spherical harmonics of even order 0 and 2. Hence, these harmonics represent the even information of 2D structures. Therefore, we are motivated to construct a tensor $T_e$, which is related to the Hessian matrix. This tensor is called a curvature tensor, because it is similar to the curvature tensor of the second fundamental form of the differential geometry. This curvature tensor $T_e$ indicates the even information of 2D image structures and can be obtained from a tensor-valued filter $H_e$ in the frequency domain, i.e. $T_e = \mathcal{F}^{-1}\{FH_e\}$, where $\mathcal{F}^{-1}$ means the inverse Fourier transform. Hence, the tensor-valued filter $H_e$, called the even Hessian operator reads

$$\begin{aligned} H_e &= \begin{bmatrix} \frac{H_0 + \mathrm{real}(H_2)}{2} & \frac{\mathrm{imag}(H_2)}{2} \\ \frac{\mathrm{imag}(H_2)}{2} & \frac{H_0 - \mathrm{real}(H_2)}{2} \end{bmatrix} = \frac{1}{2} \begin{bmatrix} 1+\cos(2\alpha) & \sin(2\alpha) \\ \sin(2\alpha) & 1-\cos(2\alpha) \end{bmatrix} \exp(-2\pi\rho s) \\ &= \begin{bmatrix} \cos^2(\alpha) & \frac{1}{2}\sin(2\alpha) \\ \frac{1}{2}\sin(2\alpha) & \sin^2(\alpha) \end{bmatrix} \exp(-2\pi\rho s) , \end{aligned} \tag{4}$$

where $\mathrm{real}(\cdot)$ and $\mathrm{imag}(\cdot)$ indicate the real and imaginary parts of the expressions.

In this filter, two components $\cos^2(\alpha)$ and $\sin^2(\alpha)$ can be considered as two angular windowing functions. These angular windowing functions provide a measure of the angular distance. From them, two perpendicular i1D components of the 2D image, oriented along the $x$ and $y$ coordinates, can be obtained. The other component of the filter is also the combination of two angular windowing functions, i.e. $\frac{1}{2}\sin(2\alpha) = \frac{1}{2}(\cos^2(\alpha - \frac{\pi}{4}) - \sin^2(\alpha - \frac{\pi}{4}))$. These two angular windowing functions yield again two i1D components of the 2D image, which are oriented along the diagonals. These four angular windowing functions can also be considered as four differently oriented filters, which are basis functions to steer a filter. They make sure that i1D components along different orientations are extracted. Consequently, the even Hessian operator $H_e$ enables the extraction of differently oriented i1D components of the 2D image.

The conjugate Poisson kernel, which evaluates the corresponding odd information of the i1D signal, is in quadrature phase relation with the i1D signal.

Therefore, the odd representation of the curvature tensor, called the conjugate curvature tensor $T_o$, is obtained by employing the conjugate Poisson kernel to elements of $T_e$. Besides, the conjugate curvature tensor $T_o$ results also from a tensor-valued odd filter $H_o$, i.e. $T_o = h_1 * T_e = \mathcal{F}^{-1}\{H_1 H_e F\} = \mathcal{F}^{-1}\{H_o F\}$, where $h_1$ denotes the conjugate Poisson kernel in the spatial domain. Hence, the odd Hessian operator $H_o$ in the spectral domain is given by

$$H_o = \frac{1}{2}\begin{bmatrix} H_1(H_0 + \mathrm{real}(H_2)) & H_1(\mathrm{imag}(H_2)) \\ H_1(\mathrm{imag}(H_2)) & H_1(H_0 - \mathrm{real}(H_2)) \end{bmatrix} . \tag{5}$$

### 2.3 Local Amplitudes and Phases

Similar as the Hessian matrix, we are able to compute the trace and determinant of $T_e$ and $T_o$ for detecting the intrinsically one dimensional (i1D) and intrinsically two dimensional (i2D) structures. Note that 2D images can be classified into three categories according to the intrinsic dimensionality [10], a local property of a multidimensional signal. Thus, constant signals are intrinsically zero dimensional (i0D) structures, i1D signals represent straight lines or edges and i2D signals are composed of curved edges and lines, junctions, etc.

Consequently, a novel model for the i1D structures is obtained by combing the traces of $T_e$ and $T_o$, this is exactly the monogenic scale-space, as proposed in [8]

$$\mathbf{f}_{i1D}(\mathbf{x}; s) = \mathrm{trace}(T_e(\mathbf{x}; s)) + \mathrm{trace}(T_o(\mathbf{x}; s)) = t_e + \mathbf{t}_o \tag{6}$$

with $\mathbf{t}_o = [\mathrm{real}(\mathrm{trace}(T_o(\mathbf{x}; s))),\ \mathrm{imag}(\mathrm{trace}(T_o(\mathbf{x}; s)))]^T$.

Hence, the multi-scale local amplitude and local phase vector for i1D structures are given by

$$a(\mathbf{x}; s) = \sqrt{t_e^2 + \mathbf{t}_o^2} \tag{7}$$

$$\boldsymbol{\varphi}(\mathbf{x}; s) = \frac{\mathbf{t}_o}{|\mathbf{t}_o|}\mathrm{atan}\left(\frac{|\mathbf{t}_o|}{t_e}\right) , \tag{8}$$

where $\frac{\mathbf{t}_o}{|\mathbf{t}_o|}$ denotes the local orientation of the i1D structure. Correspondingly, combing the determinants of $T_e$ and $T_o$ results in a novel model for the i2D structure, which is called the generalized monogenic curvature scale-space $\mathbf{f}_{i2D}(\mathbf{x}; s)$,

$$\mathbf{f}_{i2D}(\mathbf{x}; s) = \det(T_e(\mathbf{x}; s)) + \det(T_o(\mathbf{x}; s)) = d_e + \mathbf{d}_o \tag{9}$$

with $\mathbf{d}_o = [\mathrm{real}(\det(T_o(\mathbf{x}; s))),\ \mathrm{imag}(\det(T_o(\mathbf{x}; s)))]^T$.

From it, the local amplitude for the i2D structure is obtained as

$$A(\mathbf{x}; s) = \sqrt{d_e^2 + \mathbf{d}_o^2} , \tag{10}$$

and the local phase vector takes the following form

$$\Phi(\mathbf{x}; s) = \frac{\mathbf{d}_o}{|\mathbf{d}_o|}\mathrm{atan}\left(\frac{|\mathbf{d}_o|}{d_e}\right) , \tag{11}$$

where $\frac{\mathbf{d}_o}{|\mathbf{d}_o|}$ decides the local main orientation of the i2D structure.

Since the local phase information of the i1D and i2D structures contains not only phase information but also the local orientation, the evaluation can be done in a rotation-invariant way.

## 3 Dense Optical Flow Estimation

Differential methods have become the most widely used techniques for optical flow computation. By combining the advantages of local methods and global methods, Bruhn et al. [6] proposed a new method (CLG), which could yield flow fields with 100% density and have the robustness against noise. Since the phase-based approach was shown to perform very good with the advantage of being robust against brightness change [5, 4], it is very natural to combine the advantages of the phase-based approach and the CLG method. In this section, we will adapt the CLG method into our model framework to estimate two-frame optical flow fields.

### 3.1 2D Combined Local-Global (CLG) Method

Differential methods are based on the assumption that the grey values of image sequences $f(x, y, t)$ in subsequent frames do not change over time

$$f(x + u,\, y + v,\, t + 1) = f(x, y, t)\ , \tag{12}$$

where the displacement field $[u,\, v]^T$ denotes the optical flow. Following this, the spatial CLG method aims to minimize an energy function for estimating the flow field

$$E(\mathbf{w}) = \int_{\Omega} (\psi_1(\mathbf{w}^T J_\rho(\nabla_3 f)\mathbf{w}) + \alpha\psi_2(|\nabla\mathbf{w}|^2))dxdy \tag{13}$$

with

$$\nabla = [\partial_x,\, \partial_y]^T \tag{14}$$

$$\nabla_3 := [\partial_x,\, \partial_y,\, \partial_t]^T \tag{15}$$

$$\mathbf{w} := [u,\, v,\, 1]^T \tag{16}$$

$$|\nabla\mathbf{w}|^2 := |\nabla u|^2 + |\nabla v|^2 \tag{17}$$

$$J_\rho(\nabla_3 f) := K_\rho * (\nabla_3 f \nabla_3 f^T)\ , \tag{18}$$

where $\Omega$ denotes the image domain, $\alpha$ serves as regularization parameter, $K_\rho$ means a Gaussian kernel with standard deviation $\rho$, $\psi_1(\cdot)$ and $\psi_2(\cdot)$ indicate two nonquadratic penalisers with the following form

$$\psi_i(z) = 2\beta_i^2\sqrt{1 + \frac{z}{\beta_i^2}} \quad i \in \{1,\, 2\} \tag{19}$$

with $\beta_1$ and $\beta_2$ as scaling parameters to handle outliers.

### 3.2 New Energy function with Phase Constraints

In order to combine the phase-based approach with the 2D CLG method, the classical brightness constancy assumption will be replaced by new phase constraints. Two local phase vectors of i1D and i2D structures can be derived from

the monogenic curvature tensor. One can assume that local phases of image sequences $f(x, y, t)$ in subsequent frames do not change over time. This results in the following new constancy assumptions

$$\boldsymbol{\varphi}(x+u,\, y+v,\, t+1) = \boldsymbol{\varphi}(x,\, y,\, t) \tag{20}$$
$$\Phi(x+u,\, y+v,\, t+1) = \Phi(x,\, y,\, t)\ . \tag{21}$$

For small displacements, we may perform a first order Taylor expansion yielding the optical flow constraints:

$$\boldsymbol{\varphi}_x u + \boldsymbol{\varphi}_y v + \boldsymbol{\varphi}_t = 0 \tag{22}$$
$$\Phi_x u + \Phi_y v + \Phi_t = 0\ . \tag{23}$$

Let the i1D and i2D local phase vectors be $\boldsymbol{\varphi} = [\varphi_1,\, \varphi_2]^T$ and $\Phi = [\Phi_1,\, \Phi_2]^T$, respectively, we propose to minimize the following energy function

$$E(\mathbf{w}) = \int_{\Omega} (\psi_1(\mathbf{w}^T J_\rho(\nabla_3 \boldsymbol{\varphi} + \gamma \nabla_3 \Phi)\mathbf{w}) + \alpha \psi_2(|\nabla \mathbf{w}|^2))dxdy \tag{24}$$

with

$$J_\rho(\nabla_3 \boldsymbol{\varphi} + \gamma \nabla_3 \Phi) = K_\rho * \begin{bmatrix} M_{11} & M_{12} & M_{13} \\ M_{21} & M_{22} & M_{23} \\ M_{31} & M_{32} & M_{33} \end{bmatrix} \tag{25}$$

$$M_{11} = \varphi_{1x}^2 + \varphi_{2x}^2 + \gamma(\Phi_{1x}^2 + \Phi_{2x}^2) \tag{26}$$
$$M_{12} = M_{21} = \varphi_{1x}\varphi_{1y} + \varphi_{2x}\varphi_{2y} + \gamma(\Phi_{1x}\Phi_{1y} + \Phi_{2x}\Phi_{2y}) \tag{27}$$
$$M_{13} = M_{31} = \varphi_{1x}\varphi_{1t} + \varphi_{2x}\varphi_{2t} + \gamma(\Phi_{1x}\Phi_{1t} + \Phi_{2x}\Phi_{2t}) \tag{28}$$
$$M_{22} = \varphi_{1y}^2 + \varphi_{2y}^2 + \gamma(\Phi_{1y}^2 + \Phi_{2y}^2) \tag{29}$$
$$M_{23} = M_{32} = \varphi_{1y}\varphi_{1t} + \varphi_{2y}\varphi_{2t} + \gamma(\Phi_{1y}\Phi_{1t} + \Phi_{2y}\Phi_{2t}) \tag{30}$$
$$M_{33} = \varphi_{1t}^2 + \varphi_{2t}^2 + \gamma(\Phi_{1t}^2 + \Phi_{2t}^2)\ . \tag{31}$$

In this energy function, $\gamma$ is employed to adjust the trade-off between the i1D and i2D structures. According to the new energy function, the minimizing flow field $[u,\, v]^T$ will satisfy the following Euler-Lagrange equations

$$\mathrm{div}(\psi_2'(|\nabla \mathbf{w}|^2)\nabla u) - \frac{1}{\alpha}\psi_1'(\mathbf{w}^T J_\rho(\nabla_3 \boldsymbol{\varphi} + \gamma \nabla_3 \Phi)\mathbf{w})(J_{11}u + J_{12}v + J_{13}) = 0$$
$$\mathrm{div}(\psi_2'(|\nabla \mathbf{w}|^2)\nabla v) - \frac{1}{\alpha}\psi_1'(\mathbf{w}^T J_\rho(\nabla_3 \boldsymbol{\varphi} + \gamma \nabla_3 \Phi)\mathbf{w})(J_{21}v + J_{22}u + J_{23}) = 0$$

with

$$\psi_i'(z) = \frac{1}{\sqrt{1 + \frac{z}{\beta_i^2}}} \quad i \in \{1,\, 2\}\ . \tag{32}$$

The estimation of optical flow field can thus be obtained iteratively by using an SOR [11] scheme. In our application, we take 200 iterations.

### 3.3 Computation of Phase Derivatives

In order to avoid phase wrapping, phase derivatives are computed from the filter responses in the monogenic scale-space and the generalized monogenic curvature scale-space, respectively. The spatial derivatives of i1D and i2D local phase vectors are given by

$$\nabla\boldsymbol{\varphi} = \frac{t_e \nabla \mathbf{t}_o - \mathbf{t}_o^T \nabla^T t_e}{t_e^2 + |\mathbf{t}_o|^2} \tag{33}$$

$$\nabla\Phi = \frac{d_e \nabla \mathbf{d}_o - \mathbf{d}_o^T \nabla^T d_e}{d_e^2 + |\mathbf{d}_o|^2} \ . \tag{34}$$

The temporal derivatives of these local phase vectors read

$$\boldsymbol{\varphi}_t = \frac{t_e^t \mathbf{t}_o^{t+1} - t_e^{t+1} \mathbf{t}_o^t}{|t_e^t \mathbf{t}_o^{t+1} - t_e^{t+1} \mathbf{t}_o^t|} \operatorname{atan}\left(\frac{|t_e^t \mathbf{t}_o^{t+1} - t_e^{t+1} \mathbf{t}_o^t|}{t_e^t t_e^{t+1} + \mathbf{t}_o^t \cdot \mathbf{t}_o^{t+1}}\right) \tag{35}$$

$$\Phi_t = \frac{d_e^t \mathbf{d}_o^{t+1} - d_e^{t+1} \mathbf{d}_o^t}{|d_e^t \mathbf{d}_o^{t+1} - d_e^{t+1} \mathbf{d}_o^t|} \operatorname{atan}\left(\frac{|d_e^t \mathbf{d}_o^{t+1} - d_e^{t+1} \mathbf{d}_o^t|}{d_e^t d_e^{t+1} + \mathbf{d}_o^t \cdot \mathbf{d}_o^{t+1}}\right) \ , \tag{36}$$

where $t_e^t$, $\mathbf{t}_o^t$, $d_e^t$, $\mathbf{d}_o^t$ denote the filter responses of the image frame at time $t$ and $t_e^{t+1}$, $\mathbf{t}_o^{t+1}$, $d_e^{t+1}$, $\mathbf{d}_o^{t+1}$ are the filter responses of the next image frame.

### 3.4 Multi-scale Optical Flow Estimation

The linearized optical flow constraint, stated in section 3.2, is based on the phase constancy assumption. As a consequence, it requires that $u$ and $v$ are relatively small so that the linearization holds. However, this is not always the case for an arbitrary sequence. Hence, multi-scale optical flow estimation technique should be employed to deal with large displacements.

In this paper, we use an incremental coarse to fine strategy. In contrast to the classical multi-scale approach, the estimated flow field at a coarse level is used to warp the image sequence instead of serving as initialization for the next finer scale. This compensation results in a hierarchical modification which requires to compute only small displacement. Once this is done from coarse to the finest scale, much more accurate estimation will be obtained.

Let $d\mathbf{w}^s$ denote a displacement increment of $\mathbf{w}^s$ at scale $s$, for the coarsest scale ($s = S$), the optical flow field has the initial data $\mathbf{w}^S = [0,\, 0,\, 0]^T$. Hence, $d\mathbf{w}^s$ is given by minimizing the following energy function

$$\begin{aligned} E(d\mathbf{w}^s) = \int_\Omega (\psi_1((d\mathbf{w}^s)^T J_\rho(\nabla_3 \boldsymbol{\varphi}(\mathbf{x} + \mathbf{w}^s) + \gamma \nabla_3 \Phi(\mathbf{x} + \mathbf{w}^s)) d\mathbf{w}^s) \\ + \alpha \psi_2(|\nabla(\mathbf{w} + d\mathbf{w}^s)|^2)) dx dy \ , \end{aligned} \tag{37}$$

where $\mathbf{x} = [x,\, y,\, t]^T$ and $\mathbf{w}^{s+1} = \mathbf{w}^s + d\mathbf{w}^s$. Note that local phase vectors will be warped as $\boldsymbol{\varphi}(\mathbf{x} + \mathbf{w}^s)$ and $\Phi(\mathbf{x} + \mathbf{w}^s)$ via bilinear interpolation. Final result will be obtained when the minimization is done to the finest scale.

## 4 Experimental Results

In order to evaluate the performance of the proposed approach, optical flow estimation on both synthetic and real-world image data is given in this section. We use the so-called average angular error (AAE) [4] as the quantitative quality measure. Given the estimated flow field $[u_e,\, v_e]^T$ and the ground truth $[u_c,\, v_c]^T$, the AAE is defined as

$$AAE = \frac{1}{N}\sum_{i=1}^{N} \arccos\left(\frac{u_{ci}u_{ei} + v_{ci}v_{ei} + 1}{\sqrt{(u_{ci}^2 + v_{ci}^2 + 1)(u_{ei}^2 + v_{ei}^2 + 1)}}\right), \tag{38}$$

where $N$ denotes the total number of pixels.

The *Yosemite* sequence with clouds is employed as the synthetic data for the experiment. This sequence combines divergent and translational motion under varying illumination and hence is usually regarded as the benchmark for the optical flow estimation. Fig. 1 demonstrates the ground truth, the estimated magnitudes and optical flow fields from our approach and the 2D CLG model. It is obvious that our approach produces more accurate result than that of the 2D CLG method. Especially in the clouds region, where the illumination varies, the proposed approach shows more stable estimation. Even if we compare with 2D CLG where the intensity is replaced by the gradient, our approach also performs better.

Detail comparisons with other approaches according to the measurement AAE are given in Table 1, where STD indicates the standard deviation. Our approach demonstrates much better performance with lower AAE and STD when compared with most of the methods. When $\gamma = 0$, only i1D phase information is included for the constraint, the AAE now takes $3.37^0$, which is $1.49^0$ lower than that of the 2D CLG method. Interestingly, this result is even lower than that of the 3D CLG method. By adjust the parameter as $\gamma = 0.1$, i2D phase is also contained to strengthen the constraint. Hence, estimation with even lower error can be obtained. For this experiment, we also extend the two-frame estimation to multi-frame by adding the temporal information. Results also indicate the good performance of the proposed approach.

Even much better results have been reported in [1]. However, they do not perform a first order Taylor expansion of the intensity assumption to yield the optical flow constraint. Thus, it is very promising that our approach can also yield comparably good results by using the non-linearized constancy assumption.

For the following experiments, we simply focus on two-frame flow field estimation. To investigate the robustness of our approach against noise, the 8th frame of the *Yosemite* sequence is degraded with additive Gaussian noise.

The noise contaminated image (signal noise ratio: SNR=10dB) and the estimated flow field are shown in Fig. 2. It is obvious that the original image is seriously degraded, nevertheless, the estimation also shows good performance with AAE=$14.16^0$. More detail information can be found in Fig. 3. When the SNR decreases from 40dB to 10dB, much more noise is added to the original image. However, the estimated result is still not very sensitive to noise. This

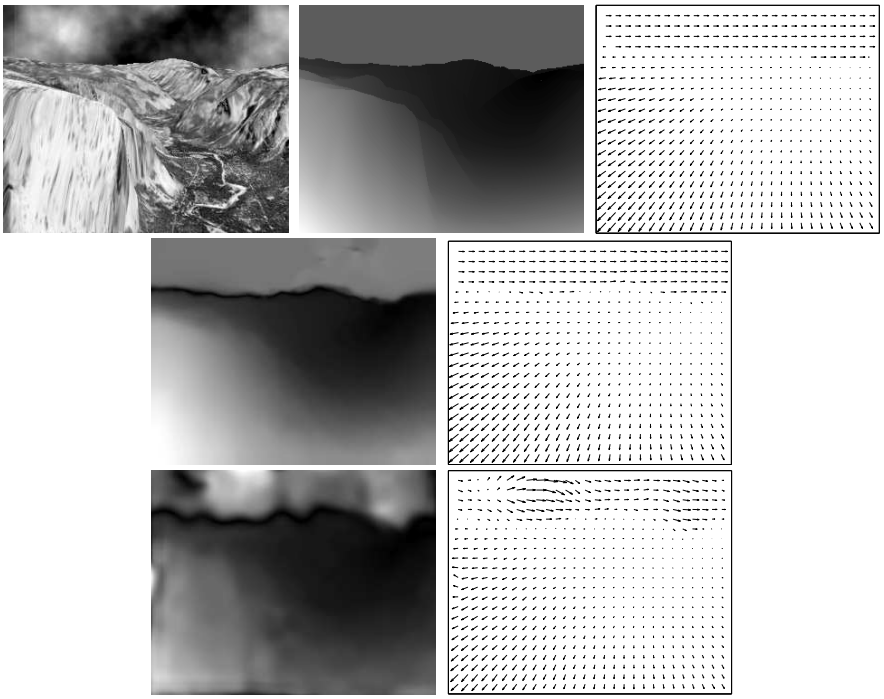

**Fig. 1.** Top row: from left to right are one frame of the Yosemite image sequence, the magnitude and flow field of the ground truth. Middle row: from left to right are the magnitude and flow field estimated from our approach. Bottom row: from left to right are the magnitude and flow field estimated from the 2D CLG method.

**Table 1.** Optical flow estimation comparisons between different approaches (100% density). AAE (average angular error), STD (standard deviation).

| Approach | AAE | STD |
|---|---|---|
| Horn/Schunck (Barron et al., 1994) [4] | $31.69^0$ | $31.18^0$ |
| Nagel (Barron et al., 1994) [4] | $10.22^0$ | $16.51^0$ |
| Uras et al. (Barron et al., 1994) [4] | $8.94^0$ | $15.61^0$ |
| 2D CLG (2005) [6] | $4.86^0$ | $8.48^0$ |
| Mémin and Pérez (1998) [12] | $4.69^0$ | $6.89^0$ |
| 3D CLG (2005) [6] | $4.17^0$ | $7.72^0$ |
| **Our 2D approach** ($\gamma = 0$) | $3.37^0$ | $8.27^0$ |
| **Our 2D approach** ($\gamma = 0.1$) | $3.25^0$ | $8.22^0$ |
| **Our 3D approach** ($\gamma = 0$) | $2.74^0$ | $7.17^0$ |
| **Our 3D approach** ($\gamma = 0.1$) | $2.67^0$ | $7.12^0$ |

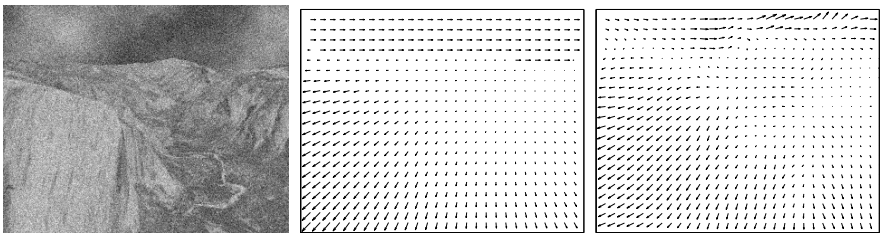

**Fig. 2.** From left to right are the noise degraded image (SNR=10dB), ground truth and the estimated flow field (AAE=$14.16^0$, STD=$12.76^0$).

indicates that employing the local method and multi-scale technique into our approach does result in a robust estimation against noise. As mentioned in [5],

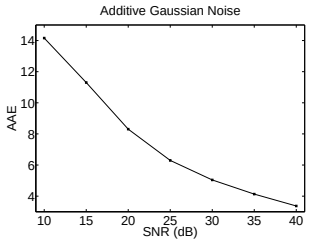


**Fig. 3.** The estimated results with respect to additive Gaussian noise change.

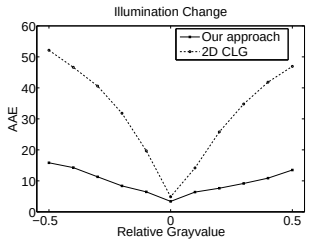


**Fig. 4.** The estimated results with respect to illumination change.

the phase-based approach has the advantage of being not sensitive to the illumination variation. Additionally, the proposed approach adapts the CLG method into the framework of the monogenic curvature tensor. As a consequence, this new method combines the advantages of phase-based approach and the CLG method. In this way, our approach should also be robust under illumination change within some limits. To this end, another experiment is conducted to test the performance of our approach for the brightness variation. Fig. 5 shows the performance comparison between our approach and the 2D CLG method under the brightness change. The 8th frame of the synthetic sequence is degraded with brighter and darker illumination changes of 50%, respectively. Experimental results denote that our approach is much more robust against illumination variation when compared with that of the 2D CLG method. To evaluate the performance of the proposed approach under illumination change in detail, the 8th frame is degraded with different brighter and darker brightness variations. The estimated AAEs with respect to the relative grayvalue changes are shown in Fig.4. Results indicate that our approach is very robust against illumination change. However, the 2D CLG method is very sensitive to it.

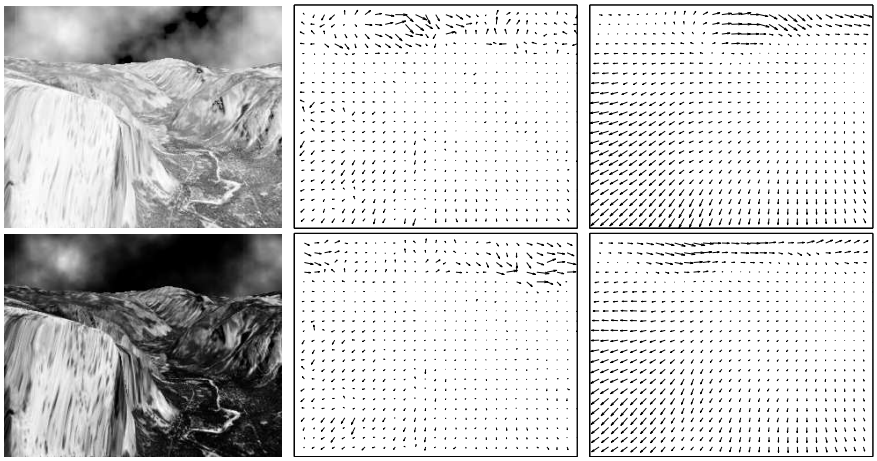

**Fig. 5.** Top row: from left to right are frame 8 degraded with brighter illumination change of 50%, estimated flow fields from the 2D CLG (AAE=$46.94^0$, STD=$39.97^0$) and our approach (AAE=$13.50^0$, STD=$17.42^0$). Bottom row: from left to right are frame 8 degraded with darker illumination variation of 50%, optical flow estimations from the 2D CLG (AAE=$52.14^0$, STD=$46.63^0$) and our method (AAE=$15.83^0$, STD=$19.71^0$).

The last experiment aims to examine the performance of the proposed approach for real image sequences. In this experiment, two sequences are used. They are the well-known Hamburg taxi sequence and the Ettlinger Tor traffic sequence [13]. Estimated flow fields are illustrated in Fig. 6. It is clear that the proposed approach also yields realistic optical flow for real-world data.

## 5 Conclusions

We present a novel approach for estimating two-frame dense optical flow field in this paper. This new approach adapts the CLG approach to the monogenic curvature tensor, a new framework which enables multi-scale local phase evaluation of i1D and i2D image structures in a rotation invariant way. Hence, our approach takes both the advantages of phase-based approach and the CLG approach. In this way, the proposed method produces accurate estimations with 100% density and is robust against noise. Compared with the intensity based approach, our method performs much better under the illumination variation.

## References

1. Papenberg, N., Bruhn, A., Brox, T., Didas, S., Weickert, J.: Highly accurate optic flow computation with theoretically justified warping. International Journal of Computer Vision **67**(2) (2006) 141–158
2. Horn, B., Schunck, B.: Determining optical flow. Artificial Intelligence **17** (1981) 185–203

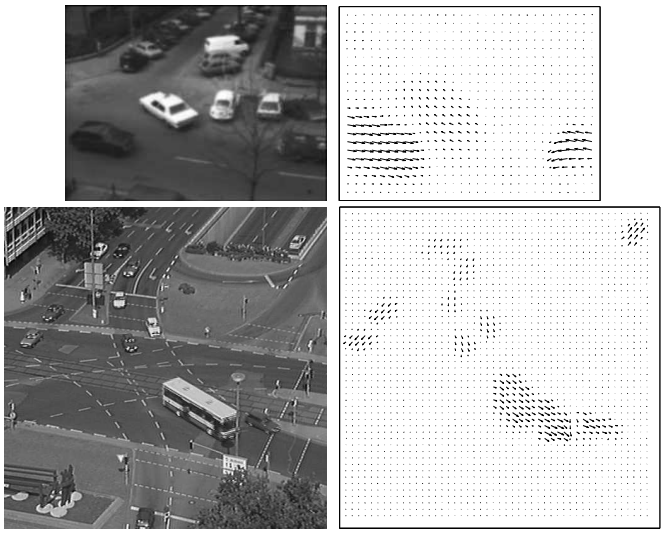

**Fig. 6.** Top row: one frame of the Hamburg taxi sequence and the estimated optical flow from our approach. Bottom row: one frame of the Ettlinger Tor traffic sequence and the flow fields from our approach.


3. Lucas, B., Kanade, T.: An iterative image registration technique with an application to stereo vision. In: Proc. 7th International Joint Conference on Artifical Intelligence, Vancouver, Canada (1981) 674–679
4. Barron, J.L., Fleet, D.J., Beauchemin, S.S.: Performance of optical flow techniques. International Journal of Computer Vision **12**(1) (1994) 43–77
5. Fleet, D.J., Jepson, A.D.: Computation of component image velocity from local phase information. International Journal of Computer Vision **5**(1) (1990) 77–104
6. Bruhn, A., Weickert, J., Schnörr, C.: Lucas/Kanada meets Horn/Schunck: Combining local and global optic flow methods. International Journal of Computer Vision **61**(3) (2005) 211–231
7. Oppenheim, A.V., Lim, J.S.: The importance of phase in signals. IEEE Proceedings **69** (May 1981) 529–541
8. Felsberg, M., Sommer, G.: The monogenic scale-space: A unifying approach to phase-based image processing in scale-space. Journal of Mathematical Imaging and Vision **21** (2004) 5–26
9. Felsberg, M., Sommer, G.: The monogenic signal. IEEE Transactions on Signal Processing **49**(12) (December 2001) 3136–3144
10. Zetzsche, C., Barth, E.: Foundamental limits of linear filters in the visual processing of two-dimensional signals. Vision Research **30** (1990) 1111–1117
11. Young, D.M.: Iterative Solution of Large Linear Systems. Academic Press (1971)
12. Mémin, E., Pérez, P.: A multigrid approach for hierarchical motion estimation. In: Proc. 6th International Conference on Computer Vision, Bombay, India, Narosa Publishing House (Jan. 1998) 933–938
13. Nagel, H.H.: Ettlinger tor traffic sequence. Available at `http://i21www.ira.uka.de/image_sequences/`